J Mater Sci (2011) 46:2685–2694
DOI 10.1007/s10853-010-5135-7

Effect of mischmetal modification treatment on the microstructure, tensile properties, and fracture behavior of Al-7.0%Si-0.3%Mg foundry aluminum alloys

Man Zhu · Zengyun Jian · Lijuan Yao · Cuixia Liu · Gencang Yang · Yaohe Zhou

Received: 25 July 2010 / Accepted: 2 December 2010 / Published online: 14 December 2010

Abstract The influence of 0.1–1.0 wt% mischmetal (MM) additives on the microstructures, tensile properties, and fracture behavior of A356 alloys were investigated in detail under the as-cast condition. Experimental results show that, after introducing a small amount of MM, grain coarsening occurred, the eutectic silicon was well modified, and RE-containing intermetallic compounds containing Al, Si, Mg, La, and Ce elements were formed. The size, shape, and distribution of RE-containing compounds are also studied. Tensile tests revealed that MM addition decreases the tensile strength and ductility of the materials. The fracture path goes through the interdendritic regions containing eutectic silicon and RE-containing compounds.

Introduction

Aluminum alloys with silicon as a major alloying ingredient are the most important commercial casting alloys. Hypoeutectic cast A356 alloy, having excellent castability, good weldability, pressure tightness, and corrosion resistance, has been widely used in the aircraft structures, automotive, and engineering industry [1]. The as-cast microstructures of A356 alloy consist of coarse α-Al dendrites and eutectic silicon. The Si phase shows coarse acicular needles and it distributes randomly in the interdendritic regions, which does harm to the tensile properties. So the modification of Si phase from acicular needles to fiber is carried out to enhance the tensile properties.

Traditionally, the modification effect of eutectic silicon can be achieved by two ways [2–6]: (1) quench modification (rapid cooling), (2) chemical modification by introducing certain elements, and (3) thermal modification. Chemical modification was usually used in the industrial field. Several elements were used as a modifier, such as Na, Sr, Sb, La, and Ce. The addition of Na and Sr can change the morphology of eutectic silicon from acicular to fibrous shape. However, large amount of Sr results in the formation of Sr-rich intermetallic particles [7]. Rare earth elements, such as La, Ce, Y, and mischmetal (MM), were reported to act as an effective modifier [4, 8–13]. It is agreed that Al–Si–Mg–MM and/or Al–Si–Mg–MM–Fe intermetallic compounds can be formed after introducing a small amount of MM into the melt [8, 9]. However, details on the morphology, size, and distribution of the RE-containing intermetallic compounds were rarely reported. Besides, the influence of RE-containing intermetallic compounds on the tensile properties is not reported. In this article, rare earth elements are introduced into A356 aluminum alloy in the form of Ce-rich MM. The microstructures of as-cast A356 alloys were studied, and the morphology, size, and distribution of RE-containing intermetallic compounds were also investigated in detail. The relationship between tensile properties and microstructures were also discussed.

M. Zhu · Z. Jian · C. Liu
School of Materials and Chemical Engineering, Xi'an Technological University, Xi'an 710032, Shaanxi, People's Republic of China

M. Zhu (✉) · G. Yang · Y. Zhou
State Key Laboratory of Solidification Processing, Northwestern Polytechnical University, Xi'an 710072, Shaanxi, People's Republic of China
e-mail: zm0428@mail.nwpu.edu.cn

L. Yao
Foundry Technology, Xi'an 710005, Shaanxi, People's Republic of China

Experimental procedure

Sample preparation

In this article, the materials used were A356 aluminum alloy and Al-10 wt%RE master alloy. For A356 alloy, it contains 6.92Si-0.29Mg-0.18Ti-0.099Fe-0.0071Cu-Bal.Al (in wt%). The Al-10 wt% RE master alloy is of Ce-rich MM with its compositions containing 6.25Ce-3.52La-0.21Fe-0.01Mg-0.10Si-0.01Cu-Bal.Al, and Ce/La ratio equals to 62.5:35.2. The A356 alloy was firstly melted under an electric resistance furnace. And the melt was refined using hexachloroethane and then degassed by pure Ar. Later, a small amount of Ce-rich MM was introduced into the melt by adding Al-10%RE master alloy. The mischmetal level, ranging from 0.1 to 1.0 wt% in step of per 0.1 wt%, was added into the melt, and then the melt was stirred. The melt was kept at 725 ± 5 °C for 20 min, and then it was poured into the metal mold pre-heated at 300 °C with size of 18 mm in diameter and 130 mm in height.

Microstructural characterization

After the experiments, the above MM-modified specimens were cut and mechanically polished from the as-cast samples. The chemical compositions of the obtained specimens were determined by inductively coupled plasma atomic emission spectroscopy (ICP-AES) and the results indicated that its compositions fitted well with its nominal compositions. Phase constitution was carried out using X-ray diffraction equipment (XRD; Philips X'pert Pro) with Cu Kα as radiation and step size of 0.033°. The microstructures were characterized through optical microscope (OM; Olympus PMG) and scanning electron microscopy (SEM; Tescan Vega II) equipped with energy dispersive spectrum (EDS; Oxford Inca 350) operated at accelerated voltage of 20 kV. The average grain size was measured by linear intercept method. In order to observe the morphology of eutectic silicon, the unmodified and MM-modified A356 alloys were deeply etched using Keller's reagent. The following parameters, i.e., mean diameter, aspect ratio, roundness, and volume fraction, were used to describe RE-containing intermetallic compounds in the as-cast MM-modified samples magnified at 500 times using Image Pro Plus 6.0 software. The above parameters were defined as follows:

Mean diameter (MD): Average length of diameters measured at 2 degree intervals and passing through particle's centroid.

Aspect ratio (A): Ratio between major axis and minor axis of ellipse equivalent to the particle. $A = L_i/L_j$, where L_i, L_j represents the length of major axis and the minor axis, respectively.

Roundness (R): $R = p^2/(4\pi S)$, where p, S represent the perimeter and area of the particle, respectively. $R = 1$, if the particle is a circle, while $R > 1$ for other particles.

Tensile tests

For tensile test, the specimens were machined having 5 mm in diameter and 25 mm in gauge according the Chinese tensile testing standard of GB/T 228-2002. Tensile properties at room temperature were performed using a universal tensile testing machine (Instron 5581). For each group, four tensile test specimens were used. Each value of tensile properties was the average value of four tensile specimens. After tensile test, the tensile-fractured specimens were protected, cleaned, and then the samples were cut normal to the tensile direction. The analysis of tensile-fractured surfaces was carried out on SEM under the secondary electron imaging mode.

Results

Phase constitution

X-ray diffraction analysis was used to identify the phase constitutions of the unmodified and MM-modified A356 alloys. The unmodified A356 alloy contains α-Al and Si two phases, as shown in Fig. 1. After adding 0.5 wt% MM, three phases, α-Al, Si, and AlCe, were identified. Although the composition, size, shape, and distribution of the RE-containing intermetallic compounds are quite complex and no pdf-card is found, the diffraction patterns were identified as AlCe phase. This phenomenon suggests that RE-containing intermetallic compounds are formed in the microstructure of the MM-modified samples, which is in accordance with that reported by Ravi et al. [8].

Microstructure

Figure 2a, b shows the macrostructural images of unmodified and MM-modified A356 alloys under the as-cast condition. Compared with the macrostructures of the unmodified A356 alloy, coarser grains were observed in the MM-modified A356 alloy. The grain size of unmodified A356 alloy is 1,160 μm, while it changes to 1,350 μm in the 0.5% MM-modified samples. Detailed analysis on the α-Al dendrites is given in Fig. 2c, d. For the unmodified A356 alloy, there exist coarse dendrites with long primary arms. However, after introducing 0.5 wt% MM, the authors observed that the α-Al grains are not refined but coarsened. After modification, well developed α-Al dendrites with longer primary arms and secondary arms were present in Fig. 2d. The results indicated that MM addition leads to

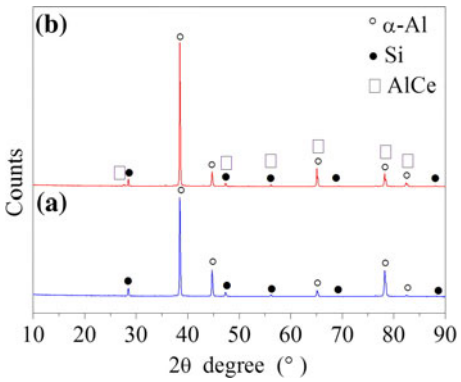

Fig. 1 The XRD patterns of the A356 alloys. (*a*) Unmodified, (*b*) 0.5 wt% MM modified

grain coarsening of primary α-Al grains and the dendritic structure is not refined.

Figure 3a gives the morphology of eutectic silicon of the unmodified A356 alloy, which reveals acicular-like in shape. The eutectic silicon, ranging from 5 to 200 μm, distributes randomly along the interdendritic regions. The MM additive produces modification effect and modification efficiency depends on the addition level of MM. As can be seen from Fig. 3b, c, when the MM addition is lower or equal to 0.2 wt%, the sizes of eutectic silicon are reduced obviously, while its morphology shows a mixture of acicular and fiber-like in shape. As the addition level of MM increases to 0.3 wt%, fine fiber-like eutectic silicon can be obtained in the microstructure (Fig. 3d). When the addition level of MM is further increased to 1.0 wt%, similar modification effect with fine fiber-like eutectic silicon is also found in Fig. 3e, f. Based on the experimental results, it can be found that minor MM (≤0.2 wt%) results in partial modification, while more MM additive (0.3– 1.0 wt%), produces full modification. The modification effect is associated with the addition of rare earth elements. The atom ratio of La:Si and Ce:Si is 1.59 and 1.56, respectively. According to the modification theory of impurity induced twinning suggested by Lu et al. [6], the impurity atoms, rare earth elements La and Ce, are adsorbed upon the silicon liquid growth front, thus, preventing the attachment of silicon atoms to the crystal. The modification is effective at growth rates where silicon normally grows anisotropically. Furthermore, the adsorbed impurity atoms of appropriate size induce twinning by altering the stacking sequence of atomic layers as the newly added layers seek to grow around the adsorbed impurity atoms. The increase of twin density changes the growth pattern of silicon, and the growth along {111} in silicon is restricted. Thus, eutectic silicon fiber is formed after modification.

Effect of modifier content on morphology, distribution, and composition of RE-containing intermetallic compounds

La and Ce react with Al to form the intermetallic compounds Al_4La, AlCe, Al_2Ce, $A_{11}Ce_3$, and La and Ce can also react

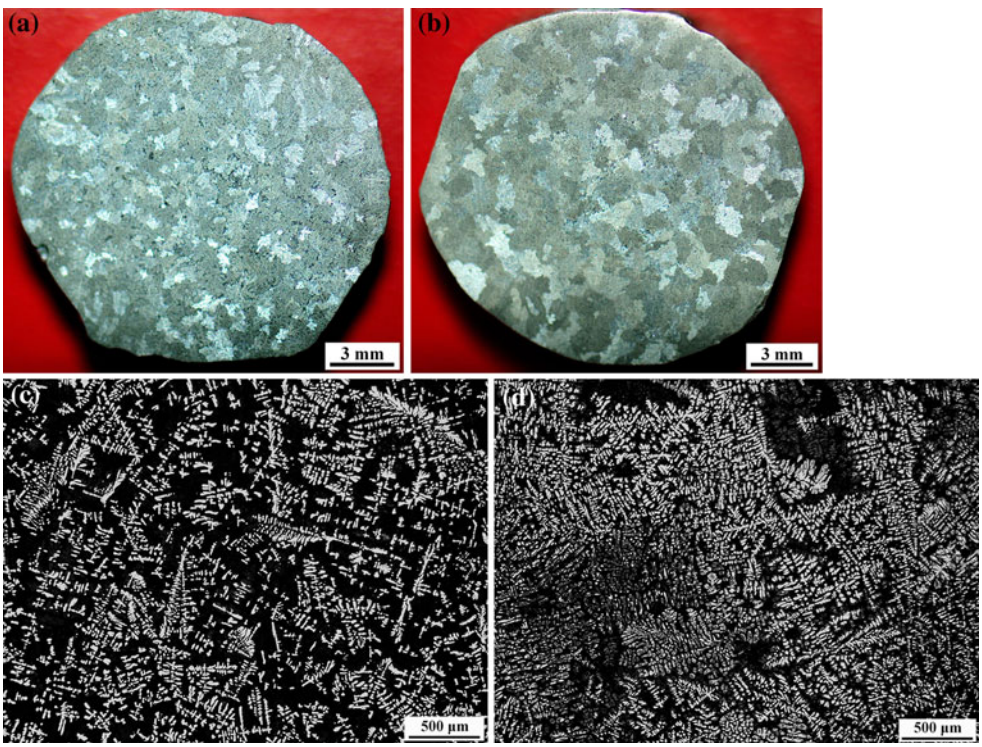

Fig. 2 Macrosctructural images of the unmodified (**a**, **c**) and 0.5 wt% MM-modified (**b**, **d**) A356 alloys. (Deeply etch using Keller's reagent)

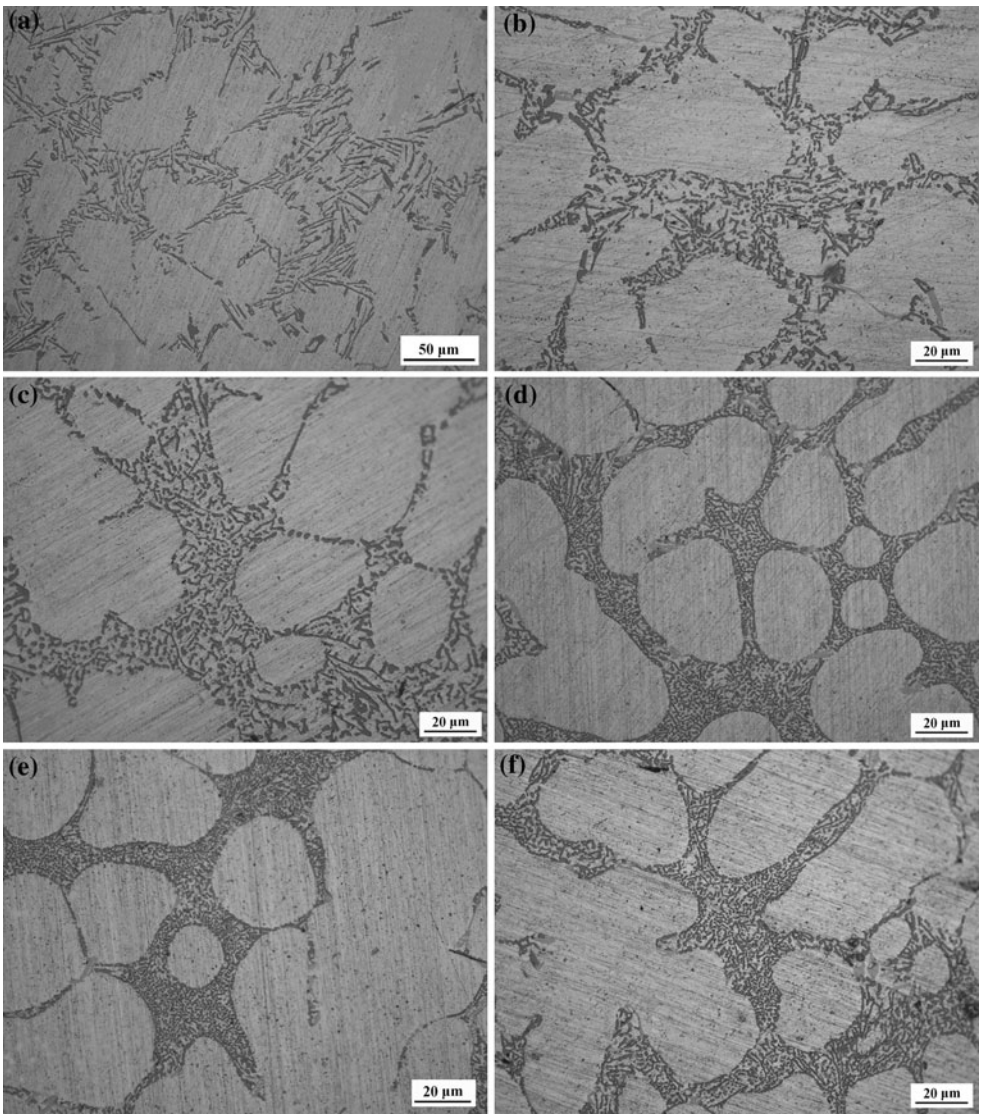

Fig. 3 Optical microstructures showing the morphology of eutectic silicon of the A356 alloys. **a** Unmodified, **b** 0.1% MM, **c** 0.2% MM, **d** 0.3% MM, **e** 0.5% MM, and **f** 1.0% MM

with the precipitating Si to form intermetallic compounds such as Ce_2Si, Ce_3Si, CeSi, and La_2Si. However, intermetallic compounds containing Al, Si, La, and Ce were formed when Ce-rich MM is introduced into the Al melt. The morphology, size, and distribution of RE-containing intermetallic compounds in the MM-modified A356 alloy are examined under the backscattered electron mode (BSE) by SEM, and the BSE images are given in Fig. 4. It can be found that these RE-containing intermetallic compounds distribute along the interdendritic regions. As the MM addition increases from 0.1 to 1.0 wt%, the relative amount of RE-containing intermetallic compounds increases. Adding quite a small amount of MM (0.1 wt%), as shown in Fig. 4a, they are formed in the microstructures with spot-like in shape. When MM addition increases, shown in Fig. 4b, c, it is found that they mainly reveal two morphologies: short lath-like and blocky-like. When MM addition increases to 0.8 wt%, small amount of RE-containing intermetallic compounds with coarse blocky-like (20–40 μm) and coarse lathy-like ((1.0–2.5) × (7–26) μm), as arrowed in Fig. 4d, can be observed in the microstructures.

The key parameters, i.e., mean diameter, aspect ratio, roundness, and volume fraction, describing the RE-containing intermetallic compounds in the MM-modified A356 alloy are summarized in Table 1. From Table 1, as the addition level of MM increases, the average value of mean diameter increases from 3.42 to 5.44 μm, and at the same time, the volume fraction increases from 0.81 to 4.25%. In addition, the average values of aspect ratio and roundness, ranging 2.37–2.71 and 2.14–2.93, respectively, are greater than 2, which mean that they are not regular.

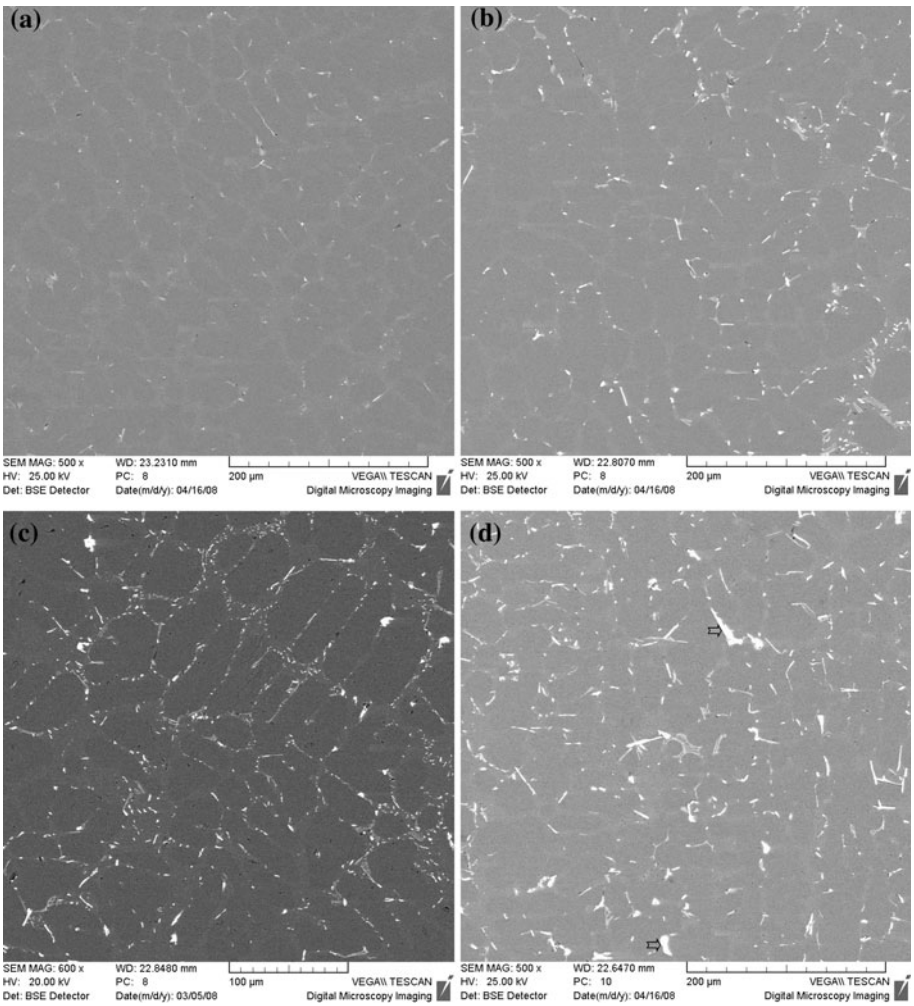

Fig. 4 Backscattered electron (BSE) images showing the microstructures of the MM-modified A356 alloy. **a** 0.1% MM, **b** 0.2% MM, **c** 0.5% MM, and **d** 0.8% MM

From the above analysis, the RE-containing intermetallic compounds mainly reveal three typical morphologies: spot-like, blocky-like, and lathy-like. The compositions on different morphologies of RE-containing intermetallic compounds are listed in Table 2 using EDS analysis. Based on the EDS results, it can be concluded that the RE-containing intermetallic compounds contain Al, Si, Mg, La, and Ce elements. From Table 2, the RE-containing intermetallic compounds, with spotted-like and blocky-like, have the same compositions containing less La and Ce. However, the compositions of the RE-containing intermetallic compounds with lathy-like, coarse blocky-like, and coarse lathy-like are almost the same, containing more La and Ce and less Al and Si.

Room-temperature tensile properties

The ultimate tensile strength (UTS), yield strength (YS), and percentage elongation (EL) of the unmodified and MM-modified A356 alloys under as-cast condition were determined. Table 3 shows typical tensile properties (UTS, YS, and EL) of the unmodified and MM-modified A356 alloys. From Table 3, it can be seen that the values of UTS, YS, and EL are 164.09, 92.73 MPa, and 4.03% for the unmodified A356 alloy, respectively. However, MM addition decreases tensile strength and elongation percentage. The values of UTS, YS, and EL are reduced by 19.75, 10.17, and 33.50%, respectively after adding 0.5 wt% MM.

Tensile fractured surfaces of as-cast specimens

In the MM-modified A356 alloy, eutectic silicon and RE-containing intermetallic compounds in the microstructures are two important particles. The size, shape factor, distribution, and the relative amount of these two particles affect the fracture behavior. If the MM-modified A356 alloys are not etched, the RE-containing intermetallic compounds with white color were observed clearly and eutectic silicon revealed gray with no obvious morphology. However, when the samples are etched deeply, it clearly showed the morphology of eutectic silicon, while the RE-containing

Table 1 Key parameters describing the characteristics of the RE-containing intermetallic compounds in the MM-modified A356 alloys

MM additive (x wt%)	Value	Mean diameter (μm)	Aspect ratio	Roundness	Volume fraction (%)
0.1	Minimum value	1.18	1.03	1.00	0.81
	Maximum value	9.68	14.95	18.12	
	Average value	3.42	2.52	2.61	
0.2	Minimum value	1.87	1.05	1.00	2.35
	Maximum value	22.77	10.13	31.51	
	Average value	4.10	2.37	2.86	
0.5	Minimum value	1.68	1.01	1.00	3.25
	Maximum value	23.07	11.94	17.56	
	Average value	4.64	2.71	2.14	
0.8	Minimum value	1.18	1.03	1.00	4.25
	Maximum value	39.50	11.70	53.33	
	Average value	5.44	2.64	2.93	

Table 2 Elemental composition of the RE-containing intermetallic compounds identified by EDS

Morphology	Element composition of RE-containing intermetallic compounds					
		Al *Kα*	Si *Kα*	Mg *Kα*	La *Lα*	Ce *Lα*
Spot-like	at.%	65.89–84.49	11.40–28.82	0.73–2.16	0.89–2.31	1.97–5.28
	wt%	49.96–73.38	10.37–26.30	0.57–1.68	4.05–8.95	8.97–20.67
Blocky-like	at.%	61.61–86.02	10.74–30.60	0.52–2.86	0.07–1.81	0.06–4.56
	wt%	48.23–84.56	11.00–24.93	0.44–2.54	0.03–7.29	0.26–18.55
Lathy-like	at.%	59.38–62.78	24.97–32.20	0.82–4.94	2.36–2.57	4.96–5.04
	wt%	44.65–47.87	19.81–25.20	0.55–3.40	9.28–9.93	19.64–19.67
Coarse blocky- and lathy-like	at.%	37.26–58.92	31.28–44.48	0.32–2.77	3.08–6.33	6.08–11.62
	wt%	21.08–42.24	23.24–26.19	0.16–1.57	11.37–18.43	22.65–34.14

Table 3 Mechanical properties of the as-cast MM-modified A356 alloys

MM additive (wt%)	UTS (MPa)	YS (MPa)	EL (%)
0	164.09 ± 9.25	92.73 ± 2.62	4.03 ± 0.55
0.2	153.59 ± 7.60	85.70 ± 3.43	3.28 ± 0.45
0.5	131.69 ± 8.20	83.30 ± 3.86	2.68 ± 0.40
1.0	160.98 ± 9.85	88.07 ± 1.95	3.57 ± 0.57

compounds are eliminated because of the corrosion-resistance difference between these two particles. So, in order to observe the cracking of eutectic silicon and RE-containing intermetallic compounds, the MM-modified samples should be deeply etched and not be etched, respectively.

Here, take a 0.2 wt% MM-modified A356 alloy for example, the fracture surfaces parallel and perpendicular to the tensile direction are shown in Fig. 5. The fracture surfaces are covered by cleavage planes and minor dimples (Fig. 5a), suggesting that it belongs to a brittle fracture mode. From the fracture examination, it can be found that MM addition cannot enhance the ductility of the A356 alloy. During the tensile fracture in the MM-modified A356 alloy, the cracking behavior of eutectic silicon and RE-containing intermetallic compounds from the longitudinal sections was shown in Fig. 5b, c under BSE mode. The BSE results show that the larger and more elongated particles, e.g., eutectic silicon and RE-containing intermetallic compounds, are prone to crack first, while the smaller particles remain uncrack. This is because the larger particles have a lower fracture stress because of larger defects, and the elongated particles generate higher stresses, which makes a higher probability of cracking [14]. In the fractured surfaces shown in Fig. 5b, the fracture or debonding of eutectic silicon can be observed. Multiple of cracks in eutectic silicon can also be observed near the fracture surfaces. The larger and more elongated eutectic silicon has the tendency to fracture first, while no cracks are observed in the small and rounded eutectic silicon. The cracking in eutectic silicon may occur in the center, near the end, or in the narrow region. Similar behavior of cracking behavior of eutectic silicon can be found in Reference [14–19].

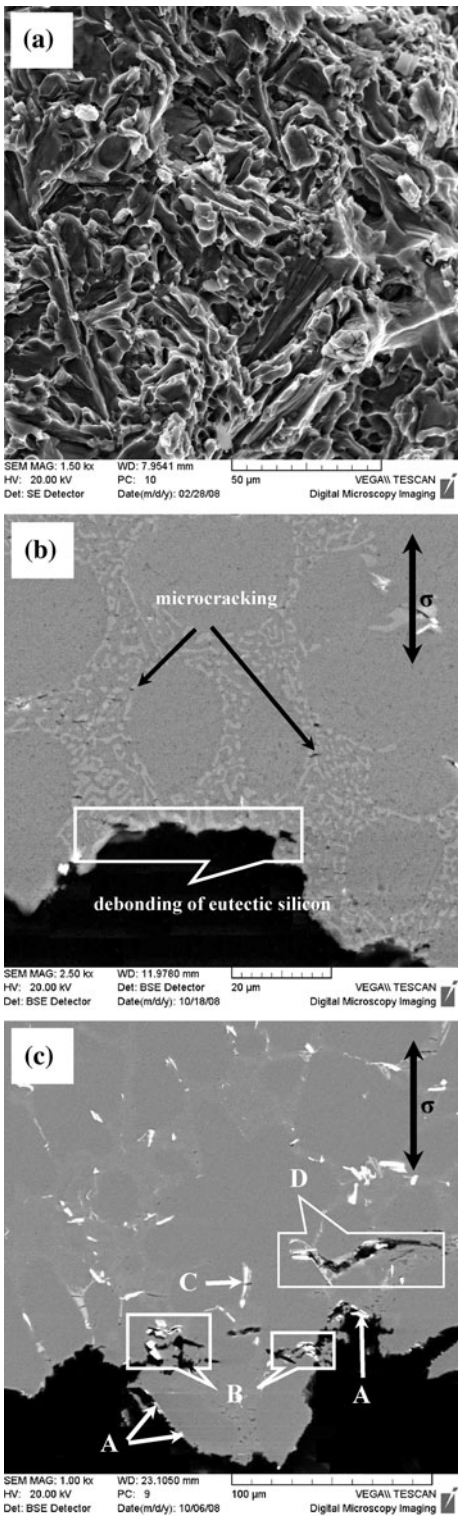

Fig. 5 Fracture analysis of as-cast A356 alloy modified by 0.2 wt% MM. **a** Perpendicular section, **b**, **c** Longitudinal section

When the 0.2 wt% MM-modified A356 alloy is deeply etched (Fig. 5c), the fracture path goes through RE-containing intermetallic compounds in the interdendritic regions. The fracture or debonding of RE-containing intermetallic compounds (A) can be seen in the fracture area. Near the fracture surfaces, lots of microcracks in the RE-containing intermetallic compounds (B, C, and D) are also clearly observed. As shown in Table 1, the average values of aspect ratio and roundness of RE-containing intermetallic compounds are greater than 2, which mean that they may have higher probability to crack. The crack behavior of the RE-containing intermetallic compounds is quite in accordance with that of eutectic silicon. Regardless of the particles orientation, the cracks in two particles are all perpendicular to the applied tensile strength, suggesting that cracking occurs due to the development of tensile stress. Besides these, the voids may play an important role in the tensile failure process. As arrowed by B, D in Fig. 5c, the fracture and cracks in eutectic silicon and RE-containing intermetallic compounds, void growth and coalescence, and the linkage of cracks in interdendritic eutectic silicon and RE-containing intermetallic compounds (D) can be observed. These phenomena mean that the tensile crack paths tend to propagate along the clusters of eutectic silicon and RE-containing intermetallic compounds.

Discussion

Grain coarsening behavior

It is generally accepted that rare earth addition has grain refinement efficiency on the Al alloys. The constitutional supercooling theory was used to explain grain refinement. Because the distribution coefficient of solute RE (RE = La, Ce) is less than 1 and solute atoms RE are enriched in the liquid ahead of the solid/liquid interface during the solidification process. The produced constitutional supercooling leads to fine dendritic structure and grain refinement. Ravi et al. [8] proved this behavior of grain refinement. However, the macrostructural study showed that small amount of Ce-rich MM into A356 alloy does not lead to grain refinement (Fig. 2). On the contrary, it causes considerable coarsening. Similar behavior was reported when beryllium was introduced into magnesium alloys [20].

The rare earth elements were introduced into the Al melt in the form of Al-10%RE binary alloy. In the Al-10%RE binary alloy, it contains two crystalline phases, $Al_{11}RE_3$ and Al_3RE (RE = La, Ce). According to Al-La and Al–Ce binary phase diagrams, Al_3Ce and Al_3La are the high temperature phases, and $Al_{11}Ce_3$ and $Al_{11}La_3$ are the low temperature phases. The precipitation temperatures of $Al_{11}Ce_3$ and $Al_{11}La_3$ are both 640 °C, which are higher than that of α-Al primary phase. It appears that, regardless of what these nucleant particles may be, MM addition can poison or considerably degrade the potency of heterogeneous nucleant particles. The results also confirmed that,

although the RE-containing intermetallic compounds are the final reaction products, they cannot act as effective nucleation sites at all. However, the mechanisms of rare earth elements in the Al melt are quite complex and still remain a problem. One possible explanation is associated with the liquid–solid freezing range. MM addition leads to depression of eutectic silicon nucleation temperature [13, 21]. Thus, it enlarges the liquid–solid freezing range. So, there is enough time to α-Al dendrites to grow, which leads to grain coarsening.

Eutectic growth

In order to observe the details of eutectic silicon, the deeply etched unmodified and MM-modified as-cast A356 alloys, were performed under secondary electron imaging mode by SEM. For the unmodified sample, as is shown in Fig. 6a, eutectic silicon reveals interconnected plate-like. During the solidification in the unmodified A356 alloy, eutectic solidification occurs in two stages-nucleation and growth. Once the eutectic silicon is nucleated, it then grows ahead of the advancing solid/liquid interface to form a continuous network. The eutectic silicon is an irregular and loosely coupled eutectic, and silicon is believed to be the leading phase in eutectic silicon [21]. Unmodified silicon should grow in a faceted manner in specific directions, and it tends to reveal an unbranched, plate-like morphology (Fig. 6a). After modification, as is shown in Fig. 6b, it reveals fine branches with its tips of half-spheroid in shape in the MM-modified samples. These phenomena suggest that, after modification, it grows non-facetted. In the MM-modified alloy, silicon does not grow ahead of the aluminum phase. After modification, the twin density in silicon crystal increases obviously, which makes the branching occur during the silicon growth. The eutectic silicon in the MM-modified alloy nucleates at the outer surface of the sample and grows toward inwardly, while that in the unmodified alloy nucleates throughout the specimen and grows randomly within the melt [22].

Strengthening mechanisms

Tensile results proved that MM additions lowered UTS, YS, and EL of the materials. It can be ascribed to the combination effect of the size, shape, and distribution of α-Al dendrites, eutectic silicon, and RE-containing intermetallic compounds.

As shown in Fig. 2, MM additive causes grain coarsening behavior, which decreases the yield strength of the materials. Before modification, the coarse acicular eutectic silicon provides convenient paths for the crack to easily debond or cut through, while the MM-modified eutectic silicon has higher fracture strength and it exerts more resistance to crack growth [15]. After modification, eutectic silicon changes into small rounded fiber and stress concentration can be reduced, which does good to the improvement of the ductility of A356 alloys. The formation of RE-containing intermetallic compounds consumed a small amount of Al and Si elements. The reduced tensile properties in the MM-modified A356 alloys are ascribed to the existence of RE-containing intermetallic compounds which are brittle and thermodynamically stable distributed in the interdendritic regions. And as the MM additive increases, the relative amount of RE-containing intermetallic compounds increases. So, the tensile properties in the MM-modified A356 alloy are influenced. It was also confirmed that the formation of RE-containing intermetallic compounds decreases the tensile properties of A356 alloy [19].

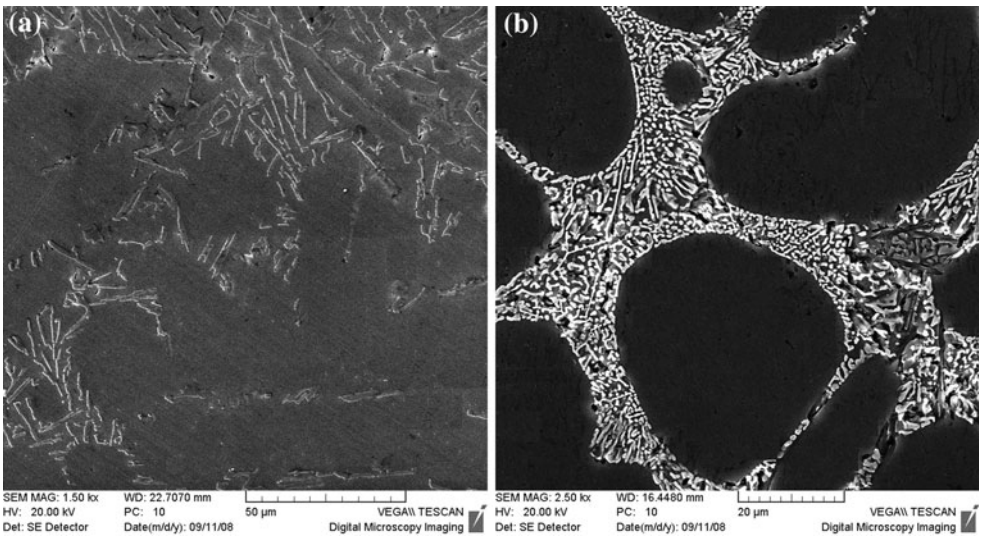

Fig. 6 The morphology of eutectic silicon in the as-cast A356 alloys deeply etched using Keller's reagent. **a** Unmodified, **b** 0.5 wt% MM modified

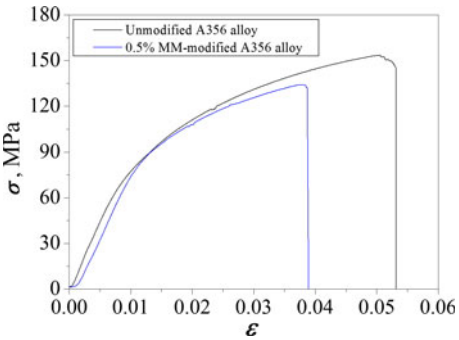

Fig. 7 Stress–strain curves of the unmodified and 0.5% MM-modified A356 alloys

Fracture mechanisms

Figure 7 gives the stress–strain curves of unmodified and 0.5 wt% MM-modified alloys. On comparison between these two alloys, it can be found that the stress–strain curve of the MM-modified alloy is lower than that of the unmodified alloy. This phenomenon revealed that MM addition results in lower stress to cause the specimen to crack. The combination effects of fracture and debonding of eutectic silicon and RE-containing intermetallic compounds (Fig. 5) are key factors to the failure process of the MM-modified A356 alloys.

It is generally accepted that the damage process of A356 alloy consists of three mixed events: (1) particle cracking, (2) microcrack formation and growth, and (3) local linkage of microcracks [14]. However, for the MM-modified specimens, the existence of RE-containing intermetallic compounds also influences its fracture behavior. During plastic deformation, stresses are imposed by the matrix on the particles in the microstructures. Then, internal stresses will be induced in the eutectic silicon and RE-containing intermetallic compounds due to inhomogeneous deformation in the MM-modified A356 alloy. After the internal stresses in the particles approaches the particle fracture stresses, the particle cracks. When the deformation proceeds, more particles will be cracked and the existing cracks will be widened. The linkage of the microcracks leads to the final damage.

Conclusions

The microstructures, tensile properties, and the fracture behavior in the MM-modified A356 alloys were investigated as a function of the addition level of Ce-rich MM. The main conclusions can be drawn as follows.

(1) The microstructures of the as-cast MM-modified A356 alloys consist of α-Al, eutectic silicon, and Al–Si–Mg–La–Ce phases. Ce-rich MM was found to hinder the grain refinement of A356 alloys. The mechanism concerning grain coarsening ability of Ce-rich MM in A356 alloys remains unclear. It appears that $Al_{11}RE_3$, Al_3RE, and RE-containing intermetallic compounds cannot act as potential heterogeneous nucleate sites for primary α-Al phases.

(2) The modification effect depends on the addition level of Ce-rich MM. Minor amount of Ce-rich MM (≤0.2 wt%) results in partial modification, while more than 0.3 wt% MM leads to full modification.

(3) Ce-rich MM additive, ranging from 0.1 to 1.0%, results in the formation of undesirable intermetallic compounds containing Al, Si, Mg, La, and Ce elements. As the MM additive increases, the size and relative amount of these compounds increases, while the shape of them transits from spotted-like into lathy-like and blocky-like. EDS results indicate that the MM (La, Ce) contents in the blocky-like RE-containing intermetallic compounds are more than that in the spotted-like compounds.

(4) The additive of Ce-rich MM lowered the tensile strength and elongation percentage in the MM-modified A356 alloys. This phenomenon is ascribed to the following two factors: (1) grain coarsening, and (2) formation of RE-containing intermetallic compounds.

(5) The fracture path goes through the interdendritic region composed by eutectic silicon and RE-containing intermetallic compounds. Fracture or debonding of eutectic silicon and RE-containing intermetallic compounds, formation and growth of voids around these particles, and subsequent interlinkage of the voids leads to crack propagation in the interdendritic regions, which make fracture failure of the MM-modified A356 alloys occur.

Acknowledgement The authors thank the National Natural Science Foundation of China (Grant no. 50571081) for financial support.

References

1. John EH (1984) Aluminum: properties and physical metallurgy. American Society for Metals, Metals Park, OH, p 320
2. Nafisi S, Ghomashchi R (2006) Mater Sci Eng A 415:273
3. Hurley TJ, Atkinson RG (1985) AFS Trans 93:291
4. Hellawell A (1970) Prog Mater Sci 15:3
5. Closset A, Gruzleski JE (1982) Metall Trans A 13:945
6. Lu SZ, Hellawell A (1987) Metall Trans A 18:1721
7. Miresmaeili SM, Campbell J, Shabestari SG, Boutorabi SMA (2005) Metall Mater Trans A 36:2341
8. Ravi M, Pillar UTS, Pai BC, Damodaran AD, Dwarakadasa ES (1994) Metall Mater Trans A 27:1283
9. Ravi M, Pillar UTS, Pai BC, Damodaran AD, Dwarakadasa ES (2002) Metall Mater Trans A 33:391

10. El Sebaie O, Samuel AM, Samuel FH, Doty HW (2008) Mater Sci Eng A 480:342
11. Tsai YC, Chou CY, Lee SL, Lin CK, Lin JC, Lim SW (2009) J Alloys Compd 487:157
12. Nogita K, Knuutinen A, McDonald SD, Dahle KA (2004) Mater Trans 45:323
13. Knuutinen A, Nogita K, McDonald SD, Dahle AK (2001) J Light Met 1:229
14. Wang QG (2003) Metall Mater Trans A 34:2887
15. Lados DA, Apelian D, Major JF (2006) Metall Mater Trans A 37:2405
16. Ran G, Zhou JE, Wang QG (2008) J Mater Process Tech 207:46
17. Yeh JW, Liu WP (1996) Metall Mater Trans A 27:3558
18. Caceres CH, Griffiths JR (1996) Acta Mater 44:25
19. Lee K, Kwon YN, Lee S (2008) J Alloys Compd 461:532
20. Cao P, Qian M, St John DH (2004) Scr Mater 51:647
21. Lu L, Nogita K, McDonald SD, Dahle AK (2004) JOM 56:52
22. Kim CB, Heine RW (1963–1964) J Inst Met 92: 367